[CANCER RESEARCH 57, 4593–4599, October 15, 1997]

Humanization of an Anti-Vascular Endothelial Growth Factor Monoclonal Antibody for the Therapy of Solid Tumors and Other Disorders

Leonard G. Presta, Helen Chen, Shane J. O'Connor, Vanessa Chisholm, Y. Gloria Meng, Lynne Krummen, Marjorie Winkler, and Napoleone Ferrara[1]

Departments of Immunology, Process Sciences, Molecular Biology, Bioanalytical Technology and Cardiovascular Research, Genentech, Inc., South San Francisco, California 94080

ABSTRACT

Vascular endothelial growth factor (VEGF) is a major mediator of angiogenesis associated with tumors and other pathological conditions, including proliferative diabetic retinopathy and age-related macular degeneration. The murine anti-human VEGF monoclonal antibody (muMAb VEGF) A.4.6.1 has been shown to potently suppress angiogenesis and growth in a variety of human tumor cells lines transplanted in nude mice and also to inhibit neovascularization in a primate model of ischemic retinal disease. In this report, we describe the humanization of muMAb VEGF A.4.6.1. by site-directed mutagenesis of a human framework. Not only the residues involved in the six complementarity-determining regions but also several framework residues were changed from human to murine. Humanized anti-VEGF F(ab) and IgG1 variants bind VEGF with affinity very similar to that of the original murine antibody. Furthermore, recombinant humanized MAb VEGF inhibits VEGF-induced proliferation of endothelial cells *in vitro* and tumor growth *in vivo* with potency and efficacy very similar to those of muMAb VEGF A.4.6.1. Therefore, recombinant humanized MAb VEGF is suitable to test the hypothesis that inhibition of VEGF-induced angiogenesis is a valid strategy for the treatment of solid tumors and other disorders in humans.

INTRODUCTION

It is now well established that angiogenesis is implicated in the pathogenesis of a variety of disorders. These include solid tumors, intraocular neovascular syndromes such as proliferative retinopathies or AMD,[2] rheumatoid arthritis, and psoriasis (1, 2, 3). In the case of solid tumors, the neovascularization allows the tumor cells to acquire a growth advantage and proliferative autonomy compared to the normal cells. Accordingly, a correlation has been observed between density of microvessels in tumor sections and patient survival in breast cancer as well as in several other tumors (4–6).

The search for positive regulators of angiogenesis has yielded several candidates, including acidic fibroblast growth factor (FGF), bFGF, transforming growth factor α, transforming growth factor β, hepatocyte growth factor, tumor necrosis factor-α, angiogenin, interleukin 8, and others (1, 2). However, in spite of extensive research, there is still uncertainty as to their role as endogenous mediators of angiogenesis. The negative regulators thus far identified include thrombospondin (7), the M_r 16,000 NH_2-terminal fragment of prolactin (8), angiostatin (9), and endostatin (10).

Work done over the last several years has established the key role of VEGF in the regulation of normal and abnormal angiogenesis (11). The finding that the loss of even a single VEGF allele results in embryonic lethality points to an irreplaceable role played by this factor in the development and differentiation of the vascular system (11). Also, VEGF has been shown to be a key mediator of neovascularization associated with tumors and intraocular disorders (11). The VEGF mRNA is overexpressed by the majority of human tumors examined (12–16). In addition, the concentration of VEGF in eye fluids is highly correlated to the presence of active proliferation of blood vessels in patients with diabetic and other ischemia-related retinopathies (17). Furthermore, recent studies have demonstrated the localization of VEGF in choroidal neovascular membranes in patients affected by AMD (18).

The muMAb VEGF A.4.6.1 (19) has been used extensively to test the hypothesis that VEGF is a mediator of pathological angiogenesis *in vivo*. This high affinity MAb is able to recognize all VEGF isoforms (19) and has been shown to inhibit potently and reproducibly the growth of a variety of human tumor cell lines in nude mice (11, 20–23). Moreover, intraocular administration of muMAb VEGF A.4.6.1 resulted in virtually complete inhibition of iris neovascularization secondary to retinal ischemia in a primate model (24).

A major limitation in the use of murine antibodies in human therapy is the anti-globulin response (25, 26). Even chimeric molecules, where the variable (V) domains of rodent antibodies are fused to human constant (C) regions, are still capable of eliciting a significant immune response (27). A powerful approach to overcome these limitations in the clinical use of monoclonal antibodies is "humanization" of the murine antibody. This approach was pioneered by Jones *et al.* (28) and Riechman *et al.* (29), who first transplanted the CDRs of a murine antibody into human V domains antibody.

In the present article, we report on the humanization of muMAb VEGF A.4.6.1. Our strategy was to transfer the six CDRs, as defined by Kabat *et al.* (30), from muMAb VEGF A.4.6.1 to a consensus human framework used in previous humanizations (31–33). Seven framework residues in the humanized variable heavy (VH) domain and one framework residue in the humanized variable light (VL) domain were changed from human to murine to achieve binding equivalent to muMAb VEGF A.4.6.1. This humanized MAb is suitable for clinical trials to test the hypothesis that inhibition of VEGF action is an effective strategy for the treatment of cancer and other disorders in humans.

MATERIALS AND METHODS

Cloning of Murine Mab A.4.6.1 and Construction of Mouse-Human Chimeric Fab. Total RNA was isolated from hybridoma cells producing the anti-VEGF MAb A.4.6.1 using RNAsol (Tel-Test) and reverse-transcribed to cDNA using Oligo-dT primer and the SuperScript II system (Life Technologies, Inc., Gaithersburg, MD). Degenerate oligonucleotide primer pools, based of the NH_2-terminal amino acid sequences of the light and heavy chains of the antibody, were synthesized and used as forward primers. Reverse primers were based on framework 4 sequences obtained from murine light chain subgroup κV and heavy chain subgroup II (30). After PCR amplification, DNA fragments were ligated to a TA cloning vector (Invitrogen, San Diego, CA). Eight clones each of the light and

Received 5/27/97; accepted 8/16/97.

The costs of publication of this article were defrayed in part by the payment of page charges. This article must therefore be hereby marked *advertisement* in accordance with 18 U.S.C. Section 1734 solely to indicate this fact.

[1] To whom requests for reprints should be addressed, at Department of Cardiovascular Research, Genentech, Inc., 460 Point San Bruno Boulevard, South San Francisco, CA 94080. Phone: (415) 225-2968; Fax: (415) 225-6327; E-mail: Ferrara.Napoleone@gene.com.

[2] The abbreviations used are: AMD, age-related macular degeneration; bFGF, basic fibroblast growth factor; VEGF, vascular endothelial growth factor; MAb, monoclonal antibody; muMAb, murine MAb; rhuMAb, recombinant humanized MAb; CDR, complementarity-determining region.

heavy chains were sequenced. One clone with a consensus sequence for the light chain VL domain and one with a consensus sequence for the heavy chain VH domain were subcloned, respectively, into the pEMX1 vector containing the human CL and CH1 domains (31), thus generating a mouse-human chimeric F(ab). This chimeric F(ab) consisted of the entire murine A.4.6.1 VH domain fused to a human CH1 domain at amino acid SerH113, and the entire murine A.4.6.1 VL domain fused to a human CL domain at amino acid LysL107. Expression and purification of the chimeric F(ab) were identical to those of the humanized F(ab)s. The chimeric F(ab) was used as the standard in the binding assays.

Computer Graphics Models of Murine and Humanized F(ab)s. Sequences of the VL and VH domains (Fig. 1) were used to construct a computer graphics model of the murine A.4.6.1 VL-VH domains. This model was used to determine which framework residues should be incorporated into the humanized antibody. A model of the humanized F(ab) was also constructed to verify correct selection of murine framework residues. Construction of models was performed as described previously (32, 33).

Construction of Humanized F(ab)s. The plasmid pEMX1 used for mutagenesis and expression of F(ab)s in *Escherichia coli* has been described previously (31). Briefly, the plasmid contains a DNA fragment encoding a consensus human κ subgroup I light chain (VLκI-CL) and a consensus human subgroup III heavy chain (VHIII-CH1) and an alkaline phosphatase promoter. The use of the consensus sequences for VL and VH has been described previously (32).

To construct the first F(ab) variant of humanized A.4.6.1, F(ab)-1, site-directed mutagenesis (34) was performed on a deoxyuridine-containing template of pEMX1. The six CDRs were changed to the murine A.4.6.1 sequence; the residues included in each CDR were from the sequence-based CDR definitions (30). F(ab)-1, therefore, consisted of a complete human framework (VL κ subgroup I and VH subgroup III) with the six complete murine CDR sequences. Plasmids for all other F(ab) variants were constructed from the plasmid template of F(ab)-1. Plasmids were transformed into *E. coli* strain XL-1 Blue (Stratagene, San Diego, CA) for preparation of double- and single-stranded DNA. For each variant, DNA coding for light and heavy chains was completely sequenced using the dideoxynucleotide method (Sequenase; U.S. Biochemical Corp., Cleveland, OH). Plasmids were transformed into *E. coli* strain 16C9, a derivative of MM294, plated onto Luria broth plates containing 50 μg/ml carbenicillin, and a single colony selected for protein expression. The single colony was grown in 5 ml of Luria broth-100 μg/ml carbenicillin for 5–8 h at 37°C. The 5-ml culture was added to 500 ml of AP5–50 μg/ml carbenicillin and allowed to grow for 20 h in a 4-liter baffled shake flask at 30°C. AP5 media consists of 1.5 g of glucose, 11.0 g of Hycase SF, 0.6 g of yeast extract (certified), 0.19 g of $MgSO_4$ (anhydrous), 1.07 g of NH_4Cl, 3.73 g of KCl, 1.2 g of NaCl, 120 ml of 1 M triethanolamine, pH 7.4, to 1 liter of water and then sterile filtered through a 0.1-mm Sealkeen filter. Cells were harvested by centrifugation in a 1-liter centrifuge bottle at 3000 × *g*, and the supernatant was removed. After freezing for 1 h, the pellet was resuspended in 25 ml of cold 10 mM Tris, 1 mM EDTA, and 20% sucrose, pH 8.0. Two hundred fifty ml of 0.1 M benzamidine (Sigma Chemical Co., St. Louis, MO) was added to inhibit proteolysis. After gentle stirring on ice for 3 h, the sample was centrifuged at 40,000 × *g* for 15 min. The supernatant was then applied to a protein G-Sepharose CL-4B (Pharmacia Biotech, Inc., Uppsala, Sweden) column (0.5-ml bed volume) equilibrated with 10 mM Tris-1 mM EDTA, pH 7.5. The column was washed with 10 ml of 10 mM Tris-1 mM EDTA, pH 7.5, and eluted with 3 ml of 0.3 M glycine, pH 3.0, into 1.25 ml of 1 M Tris, pH 8.0. The F(ab) was then buffer exchanged into PBS using a Centricon-30 (Amicon, Beverly, MA) and concentrated to a final volume of 0.5 ml. SDS-PAGE gels of all F(ab)s were run to ascertain purity, and the molecular weight of each variant was verified by electrospray mass spectrometry.

Construction, Expression, and Purification of Chimeric and Humanized IgG Variants. For the generation of human IgG1 variants of chimeric (chIgG1) and humanized (rhuMAb VEGF) A.4.6.1, the appropriate murine or humanized VL and VH (F(ab)-12; Table 1) domains were subcloned into separate, previously described pRK vectors (35). The DNA coding for the entire light and the entire heavy chain of each variant was verified by dideoxynucleotide sequencing.

For transient expression of variants, heavy and light chain plasmids were cotransfected into human 293 cells (36) using a high efficiency procedure (37). Media were changed to serum free and harvested daily for up to 5 days. Antibodies were purified from the pooled supernatants using protein A-Sepharose CL-4B (Pharmacia). The eluted antibody was buffer exchanged into PBS using a Centricon-30 (Amicon), concentrated to 0.5 ml, sterile filtered using a Millex-GV (Millipore, Bedford, MA), and stored at 4°C.

For stable expression of the final humanized IgG1 variant (rhuMAb VEGF), Chinese hamster ovary (CHO) cells were transfected with dicistronic vectors designed to coexpress both heavy and light chains (38). Plasmids were introduced into DP12 cells, a proprietary derivative of the CHO-K1 DUX B11 cell line developed by L. Chasin (Columbia University, New York, NY), via lipofection and selected for growth in glycine/hypoxanthine/thymidine (GHT)-free medium (39). Approximately 20 unamplified clones were randomly chosen and reseeded into 96-well plates. Relative specific productivity of each colony was monitored using an ELISA to quantitate the full-length human IgG accumulated in each well after 3 days and a fluorescent dye, Calcien AM, as a surrogate marker of viable cell number per well. Based on these data, several unamplified clones were chosen for further amplification in the presence of increasing concentrations of methotrexate. Individual clones surviving at 10, 50, and 100 nM methotrexate were chosen and transferred to 96-well plates for productivity screening. One clone, which reproducibly exhibited high specific productivity, was expanded in T-flasks and used to inoculate a spinner

Table 1 *Binding of humanized anti-VEGF F(ab) variants to VEGF*[a]

Variant	Template	Changes[b]	Purpose	EC50 F(ab)-X EC_{50} chimeric F(ab)[c] Mean	SD	N
chim-F(ab)	Chimeric F(ab)		1.0			
F(ab)-1	Human FR		Straight CDR swap	>1350		2
F(ab)-2			Chimera light chain F(ab)-1 heavy chain	>145		3
F(ab)-3			F(ab)-1 light chain Chimera heavy chain	2.6	0.1	2
F(ab)-4	F(ab)-1	ArgH71Leu	CDR-H2 conformation	>295		3
		AspH73Asn	Framework			
F(ab)-5	F(ab)-4	LeuL46Val	VL-VH interface	80.9	6.5	2
F(ab)-6	F(ab)-5	LeuH78Ala	CDR-H1 conformation	36.4	4.2	2
F(ab)-7	F(ab)-5	IleH69Phe	CDR-H2 conformation	45.2	2.3	2
F(ab)-8	F(ab)-5	IleH69Phe	CDR-H2 conformation	9.6	0.9	4
		LeuH78Ala	CDR-H1 conformation			
F(ab)-9	F(ab)-8	GlyH49Ala	CDR-H2 conformation	>150		2
F(ab)-10	F(ab)-8	AsnH76Ser	Framework	6.4	1.2	4
F(ab)-11	F(ab)-10	LysH75Ala	Framework	3.3	0.4	2
F(ab)-12	F(ab)-10	ArgH94Lys	CDR-H3 conformation	1.6	0.6	4

[a] Anti-VEGF F(ab) variants were incubated with biotinylated VEGF and then transferred to ELISA plates coated with KDR-IgG (40).
[b] Murine residues are underlined; residue numbers are according to Kabat *et al.* (30).
[c] Mean and SD are the average of the ratios calculated for each of the independent assays; the EC_{50} for chimeric F(ab) was 0.049 ± 0.013 mg/ml (1.0 nM).

culture. After several passages, the suspension-adapted cells were used to inoculate production cultures in GHT-containing, serum-free media supplemented with various hormones and protein hydrolysates. Harvested cell culture fluid containing rhuMAb VEGF was purified using protein A-Sepharose CL-4B. The purity after this step was ~99%. Subsequent purification to homogeneity was carried out using an ion exchange chromatography step. The endotoxin content of the final purified antibody was <0.10 eu/mg.

F(ab) and IgG Quantitation. For quantitating F(ab) molecules, ELISA plates were coated with 2 μg/ml of goat anti-human IgG Fab (Organon Teknika, Durham, NC) in 50 mM carbonate buffer, pH 9.6, at 4°C overnight and blocked with PBS-0.5% BSA (blocking buffer) at room temperature for 1 h. Standards [0.78–50 ng/ml human F(ab)] were purchased from Chemicon (Temecula, CA). Serial dilutions of samples in PBS-0.5% BSA-0.05% polysorbate 20 (assay buffer) were incubated on the plates for 2 h. Bound F(ab) was detected using horseradish peroxidase-labeled goat anti-human IgG F(ab) (Organon Teknika), followed by 3,3′,5,5′-tetramethylbenzidine (Kirkegaard & Perry Laboratories, Gaithersburg, MD) as the substrate. Plates were washed between steps. Absorbance was read at 450 nm on a V_{max} plate reader (Molecular Devices, Menlo Park, CA). The standard curve was fit using a four-parameter nonlinear regression curve-fitting program developed at Genentech. Data points that fell in the range of the standard curve were used for calculating the F(ab) concentrations of samples.

The concentration of full-length antibody was determined using goat anti-human IgG Fc (Cappel, Westchester, PA) for capture and horseradish peroxidase-labeled goat anti-human Fc (Cappel) for detection. Human IgG1 (Chemicon) was used as standard.

VEGF Binding Assays. For measuring the VEGF binding activity of F(ab)s, ELISA plates were coated with 2 μg/ml rabbit $F(ab')_2$ to human IgG Fc (Jackson ImmunoResearch, West Grove, PA) and blocked with blocking buffer (described above). Diluted conditioned medium containing 3 ng/ml of KDR-IgG (40) in blocking buffer were incubated on the plate for 1 h. Standards [6.9–440 ng/ml chimeric F(ab)] and 2-fold serial dilutions of samples were incubated with 2 nM biotinylated VEGF for 1 h in tubes. The solutions from the tubes were then transferred to the ELISA plates and incubated for 1 h. After washing, biotinylated VEGF bound to KDR was detected using horseradish peroxidase-labeled streptavidin (Zymed, South San Francisco, CA or Sigma) followed by 3,3′,5,5′-tetramethylbenzidine as the substrate. Titration curves were fit with a four-parameter nonlinear regression curve-fitting program (KaleidaGraph; Synergy Software, Reading, PA). Concentrations of F(ab) variants corresponding to the midpoint absorbance of the titration curve of the standard were calculated and then divided by the concentration of the standard corresponding to the midpoint absorbance of the standard titration curve. Assays for full-length IgG were the same as for the F(ab)s except that the assay buffer contained 10% human serum.

BIAcore Biosensor Assays. VEGF binding of the humanized and chimeric F(ab)s were compared using a BIAcore biosensor (41). Concentrations of F(ab)s were determined by quantitative amino acid analysis. VEGF was coupled to a CM-5 biosensor chip through primary amine groups according to manufacturer's instructions (Pharmacia). Off-rate kinetics were measured by saturating the chip with F(ab) [35 μl of 2 μM F(ab) at a flow rate of 20 μl/min] and then switching to buffer (PBS-0.05% polysorbate 20). Data points from 0–4500 s were used for off-rate kinetic analysis. The dissociation rate constant (k_{off}) was obtained from the slope of the plot of $\ln(R0/R)$ *versus* time, where $R0$ is the signal at $t = 0$ and R is the signal at each time point.

On-rate kinetics were measured using 2-fold serial dilutions of F(ab) (0.0625–2 mM). The slope, K_s, was obtained from the plot of $\ln(-dR/dt)$ *versus* time for each F(ab) concentration using the BIAcore kinetics evaluation software as described in the Pharmacia Biosensor manual. R is the signal at time t. Data between 80 and 168, 148, 128, 114, 102, and 92 s were used for 0.0625, 0.125, 0.25, 0.5, 1, and 2 mM F(ab), respectively. The association rate constant (k_{on}) was obtained from the slope of the plot of K_s *versus* F(ab) concentration. At the end of each cycle, bound F(ab) was removed by injecting 5 μl of 50 mM HCl at a flow rate of 20 μl/min to regenerate the chip.

Endothelial Cell Growth Assay. Bovine adrenal cortex-derived capillary endothelial cells were cultured in the presence of low glucose DMEM (Life Technologies, Inc.) supplemented with 10% calf serum, 2 mM glutamine, and antibiotics (growth medium), essentially as described previously (42). For mitogenic assays, endothelial cells were seeded at a density of 6×10^3 cells/well in 6-well plates in growth medium. Either muMAb VEGF A.4.6.1 or rhuMAb VEGF was then added at concentrations ranging between 1 and 5000 ng/ml. After 2–3 h, purified *E. coli*-expressed $rhVEGF_{165}$ was added to a final concentration of 3 ng/ml. For specificity control, each antibody was added to endothelial cells at the concentration of 5000 ng/ml, either alone or in the presence of 2 ng/ml bFGF. After 5 or 6 days, cells were dissociated by exposure to trypsin, and duplicate wells were counted in a Coulter counter (Coulter Electronics, Hialeah, FL). The variation from the mean did not exceed 10%. Data were analyzed by a four-parameter curve fitting program (KaleidaGraph).

***In Vivo* Tumor Studies.** Human A673 rhabdomyosarcoma cells (American Type Culture Collection; CRL 1598) were cultured as described previously in DMEM/F12 supplemented with 10% fetal bovine serum, 2 mM glutamine, and antibiotics (20, 22). Female BALB/c nude mice, 6–10 weeks old, were injected s.c. with 2×10^6 tumor cells in the dorsal area in a volume of 200 μl. Animals were then treated with muMAb VEGF A.4.6.1, rhuMAb VEGF, or a control murine MAb directed against the gp120 protein. Both anti-VEGF MAbs were administered at the doses of 0.5 and 5 mg/kg; the control MAb was given at the dose of 5 mg/kg. Each MAb was administered twice weekly i.p. in a volume of 100 μl, starting 24 h after tumor cell inoculation. Each group consisted of 10 mice. Tumor size was determined at weekly intervals. Four weeks after tumor cell inoculation, animals were euthanized, and the tumors were removed and weighed. Statistical analysis was performed by ANOVA.

RESULTS

Humanization. The consensus sequence for the human heavy chain subgroup III and the light chain subgroup κ I were used as the framework for the humanization (Ref. 30; Fig. 1). This framework has been successfully used in the humanization of other murine antibodies (31, 32, 43, 44). All humanized variants were initially made and screened for binding as F(ab)s expressed in *E. coli*. Typical yields from 500-ml shake flasks were 0.1–0.4 mg F(ab).

Two definitions of CDR residues have been proposed. One is based on sequence hypervariability (30) and the other on crystal structures of F(ab)-antigen complexes (45). The sequence-based CDRs are larger than the structure-based CDRs, and the two definitions are in agreement except for CDR-H1; CDR-H1 includes residues H31–H35 according to the sequence-based definition, and residues H26–H32 according to the structure-based definition (light chain residue numbers are prefixed with L; heavy chain residue numbers are prefixed with H). We, therefore, defined CDR-H1 as a combination of the two, *i.e.*, including residues H26–H35. The other CDRs were defined using the sequence-based definition (30).

The chimeric F(ab) was used as the standard in the binding assays. In the initial variant, F(ab)-1, the CDR residues were transferred from the murine antibody to the human framework and, based on the models of the murine and humanized F(ab)s, the residue at position H49 (Ala in humans) was changed to the murine Gly. In addition, F(ab)s that consisted of the chimeric heavy chain/F(ab)-1 light chain [F(ab)-2] and F(ab)-1 heavy chain/chimeric light chain [F(ab)-3] were generated and tested for binding. F(ab)-1 exhibited a binding affinity greater than 1000-fold reduced from the chimeric F(ab) (Table 1). Comparing the binding affinities of F(ab)-2 and F(ab)-3 suggested that framework residues in the F(ab)-1 VH domain needed to be altered to increase binding.

Previous humanizations (31, 32, 43, 44) as well as studies of F(ab)-antigen crystal structures (45, 47) have shown that residues H71 and H73 can have a profound effect on binding, possibly by influencing the conformations of CDR-H1 and CDR-H2. Changing the human residues to their murine counterparts in F(ab)-4 improved binding by 4-fold (Table 1). Inspection of the models of the murine

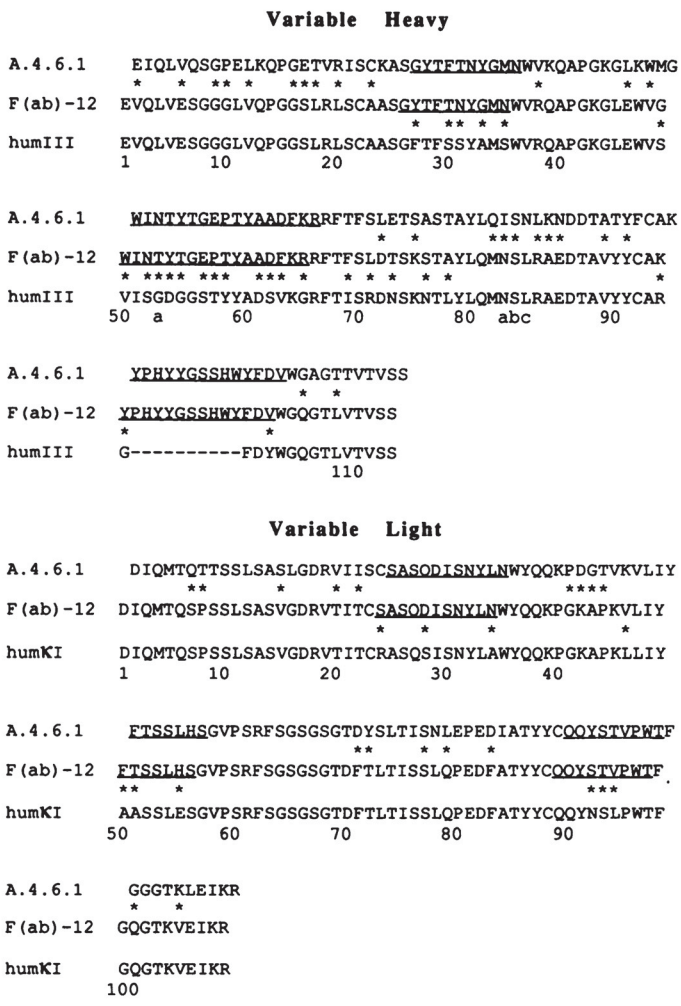

Fig. 1. Amino acid sequence of variable heavy and light domains of muMAbVEGF A.4.6.1, humanized F(ab) with optimal VEGF binding [F(ab)-12] and human consensus frameworks (*humIII*, heavy subgroup III; *humκI*, light κ subgroup I). *Asterisks*, differences between humanized F(ab)-12 and the murine MAb or between F(ab)-12 and the human framework. CDRs are *underlined*.

and humanized F(ab)s suggested that residue L46, buried at the VL-VH interface and interacting with CDR-H3 (Fig. 2), might also play a role either in determining the conformation of CDR-H3 and/or affecting the relationship of the VL and VH domains. When the murine Val was exchanged for the human Leu at L46 [F(ab)-5], the binding affinity increased by almost 4-fold (Table 1). Three other buried framework residues were evaluated based on the molecular models: H49, H69, and H78. Position H69 may affect the conformation of CDR-H2, whereas position H78 may affect the conformation of CDR-H1 (Fig. 2). When each was individually changed from the human to murine counterpart, the binding improved by 2-fold in each case [F(ab)-6 and F(ab)-7; Table 1]. When both were simultaneously changed, the improvement in binding was 8-fold [F(ab)-8; Table 1]. Residue H49 was originally included as the murine Gly; when changed to the human consensus counterpart Ala, the binding was reduced by 15-fold [F(ab)-9; Table 1].

We have found during previous humanizations that residues in a framework loop, FR-3 (30) adjacent to CDR-H1 and CDR-H2, can affect binding (44). In F(ab)-10 and F(ab)-11, two residues in this loop were changed to their murine counterparts: AsnH76 to murine Ser [F(ab)-10] and LysH75 to murine Ala [F(ab)-11]. Both effected a relatively small improvement in binding (Table 1). Finally, at position H94, human and murine sequences most often have an Arg (30). In F(ab)-12, this Arg was replaced by the rare Lys found in the murine antibody (Fig. 1), and this resulted in binding that was less than 2-fold from the chimeric F(ab) (Table 1). F(ab)-12 was also compared to the chimeric F(ab) using the BIAcore system (Pharmacia). Using this technique, the K_d of the humanized F(ab)-12 was 2-fold weaker than that of the chimeric F(ab) due to both a slower k_{on} and faster k_{off} (Table 2).

Full-length MAbs were constructed by fusing the VL and VH domains of the chimeric F(ab) and variant F(ab)-12 to the constant domains of human κ light chain and human IgG1 heavy chain. The full-length 12-IgG1 [F(ab)-12 fused to human IgG1] exhibited binding that was 1.7-fold weaker than the chimeric IgG1 (Table 3). Both 12-IgG1 and the chimeric IgG1 bound slightly less well than the original muMAb VEGF A.4.6.1 (Table 3).

Biological Studies. rhuMAb VEGF and muMAb VEGF A.4.6.1 were compared for their ability to inhibit bovine capillary endothelial cell proliferation in response to a near maximally effective concentration of $VEGF_{165}$ (3 ng/ml). In several experiments, the two MAbs were found to be essentially equivalent, both in potency and efficacy. The ED_{50}s were, respectively, 50 ± 5 and 48 ± 8 ng/ml (~0.3 nM). In both cases, 90% inhibition was achieved at the concentration of 500 ng/ml (~3 nM). Fig. 3 illustrates a representative experiment. Neither muMAb VEGF A.4.6.1 nor rhuMAb VEGF had any effect on basal or bFGF-stimulated proliferation of capillary endothelial cells (data not shown), confirming that the inhibition is specific for VEGF.

To determine whether similar findings could be obtained also in an *in vivo* system, we compared the two antibodies for their ability to suppress the growth of human A673 rhabdomyosarcoma cells in nude mice. Previous studies have shown that muMAb VEGF A.4.6.1 has a dramatic inhibitory effect in this tumor model (20, 22). As shown in Fig. 4, at both doses tested (0.5 and 5 mg/kg), the two antibodies markedly suppressed tumor growth as assessed by tumor weight measurements 4 weeks after cell inoculation. The decreases in tumor weight compared to the control group were, respectively, 85 and 93% at each dose in the animals treated with muMAb VEGF A.4.6.1 *versus* 90 and 95% in those treated with rhuMAb VEGF. Similar results were obtained with the breast carcinoma cell line MDA-MB 435 (data not shown).

DISCUSSION

The murine MAb A.4.6.1, directed against human VEGF (42), was humanized using the same consensus frameworks for the light and heavy chains used in previous humanizations (31, 32, 43, 44), *i.e.*, VκI and VHIII (30). Simply transferring the CDRs from the murine antibody to the human framework resulted in a F(ab) that exhibited binding to VEGF reduced by over 1000-fold compared to the parent murine antibody. Seven non-CDR, framework residues in the VH domain and one in the VL domain were altered from human to murine to achieve binding equivalent to the parent murine antibody.

In the VH domain, residues at positions H49, H69, H71, and H78 are buried or partially buried and probably effect binding by influencing the conformation of the CDR loops. Residues H73 and H76 should be solvent exposed (Fig. 2) and hence may interact directly with the VEGF; these two residues are in a non-CDR loop adjacent to CDRs H1 and H2 and have been shown to play a role in binding in previous humanizations (31, 32, 44). The requirement for lysine at position H94 was surprising given that this residue is arginine in the human framework (Fig. 1). In some crystal structures of F(ab)s, ArgH94 forms a hydrogen-bonded salt-bridge with

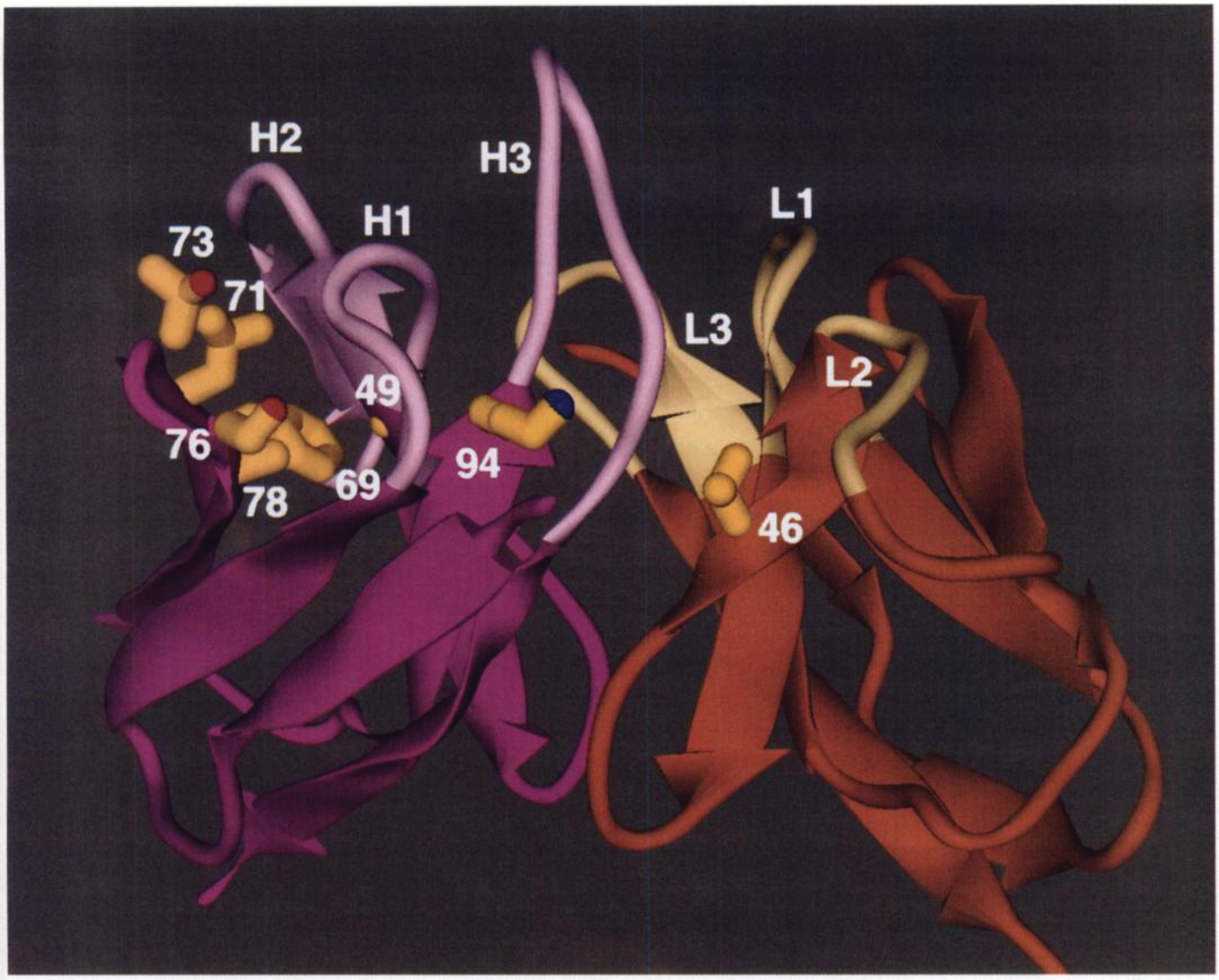

Fig. 2. Ribbon diagram of the model of humanized F(ab)-12 VL and VH domains. VL domain is shown in *brown* with CDRs in *tan*. The side chain of residue L46 is shown in *yellow*. VH domain is shown in *purple* with CDRs in *pink*. Side chains of VH residues changed from human to murine are shown in *yellow*.

Table 2 *Binding of anti-VEGF F(ab) variants to VEGF using the BIAcore system*[a]

Variant	Amount of (Fab) bound (RU)	k_{off} (s^{-1})	k_{on} ($M^{-1}s^{-1}$)	K_d (nM)
chim-F(ab)[b]	4250	5.9×10^{-5}	6.5×10^{4}	0.91
F(ab)-12	3740	6.3×10^{-5}	3.5×10^{4}	1.8

[a] The amount of F(ab) bound, in resonance units (RU), was measured using a BIAcore system when 2 μg F(ab) was injected onto a chip containing 2480 RU of immobilized VEGF. Off-rate kinetics (k_{off}) were measured by saturating the chip with F(ab) and then monitoring dissociation after switching to buffer. On-rate kinetics (k_{on}) were measured using 2-fold serial dilutions of F(ab). K_d, the equilibrium dissociation constant, was calculated as k_{off}/k_{on}.

[b] chim-F(ab) is a chimeric F(ab) with murine VL and VH domains fused to human CL and CH1 heavy domains.

AspH101 (33, 48). Substitution of lysine for arginine might conceivably alter this salt-bridge and perturb the conformation of CDR-H3.

In the VL domain, only one framework residue had to be changed to murine to optimize the humanization. Position L46 is at the VL-VH interface, where it is buried and interacts directly with CDR-H3 (Fig. 2). The requirement for murine valine (as opposed to human leucine) implies that this residue plays an important role in the conformation of CDR-H3. The necessity of retaining LysH94 in VH, which is also adjacent to CDR-H3, suggests that CDR-H3 plays a major role in the binding of the antibody to VEGF.

The humanized version with optimal binding, 12-IgG1, exhibited only a 2-fold reduction in binding compared to the parent murine antibody (Table 3). An analysis of the binding kinetics of the humanized and chimeric F(ab)s showed that both had similar off-rates but that the humanized F(ab) had a 2-fold slower on-rate (Table 2), which accounts for the 2-fold reduction in binding. However, this modest reduction in on-rate did not result in any decreased ability to antagonize VEGF bioactivity. The two anti-

Table 3 *Binding of anti-VEGF IgG variants to VEGF*[a]

Variant	IgG1/chIgG1[b] Mean	SD	N
chIgG1	1.0		2
murIgG1[c]	0.759	0.001	2
12-IgG1[d]	1.71	0.03	2

[a] Anti-VEGF IgG variants were incubated with biotinylated VEGF and then transferred to ELISA plates coated with KDR-IgG (40).

[b] chIgG1 is chimeric IgG1 with murine VL and VH domains fused to human CL and IgG1 heavy chains; the EC_{50} for chIgG1 was 0.113 ± 0.013 μg/ml (0.75 nM).

[c] murIgG1 is muMAb VEGF A.4.6.1 purified from ascites.

[d] 12-IgG1 is F(ab)-12 VL and VH domains fused to human CL and IgG1 heavy chains.

bodies had essentially identical activity, both in an endothelial cell proliferation assay and in an *in vivo* tumor model.

Interestingly, an alternative approach using monovalent phage display has been also applied to the humanization of muMAb VEGF A.4.6.1. (49). Random mutagenesis of framework residues resulted in selection of variants with significantly improved affinity compared to the initial humanized MAb with no framework changes. However, the best variant obtained by this method had a less complete restoration of the binding affinity of muMAb VEGF A.4.6.1 compared to that reported in this study (49). Clearly, this does not rule out the possibility that other applications of phage display, such as affinity maturation of the CDRs (50), may result in variants with even higher affinity.

In conclusion, protein engineering techniques resulted in virtually complete acquisition by a human immunoglobulin framework of the binding properties and biological activities of a high-affinity murine anti-VEGF MAb. In view of the nearly ubiquitous up-regulation of VEGF mRNA in human tumors (12–16) and the ability of muMAb VEGF A.4.6.1 to inhibit the *in vivo* growth of a broad spectrum of tumor cell lines (20–23), VEGF is a major target of anticancer therapy. Clinical trials using rhuMAb VEGF should allow us to test the hypothesis that inhibition of VEGF-mediated angiogenesis is an effective strategy for the treatment of several solid tumors in humans. Such trials are already under way. Other important clinical applications of rhuMAb VEGF include the prevention of blindness secondary to proliferative diabetic retinopathy (17) or AMD (18). Clearly, the success of the humanization can be ultimately judged by the degree of anti-human globulin response and and by the clinical response in patients. However, the recent report of a Phase II study where rhuMAb HER2, a humanized MAb with the same framework as rhuMAb VEGF, did not induce any anti-globulin response in breast cancer patients and also demonstrated clinical efficacy (51), makes one optimistic. The results of this (51) as well as other (52) trials raise hope that, after many disappointing results (53), progress in antibody technology, coupled with selection of better targets, will bring therapy with MAbs closer to fulfilling its promises.

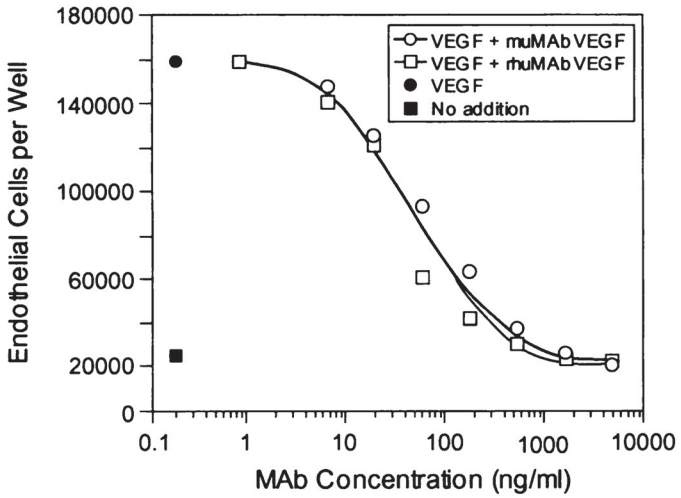

Fig. 3. Inhibition of VEGF-induced mitogenesis. Bovine adrenal cortex-derived capillary endothelial cells were seeded at the density of 6×10^3 cells/well in six-well plates, as described in "Materials and Methods." Either muMAb VEGF A.4.6.1 or rhuMAb VEGF (IgG1) was added at the indicated concentrations. After 2–3 h, $rhVEGF_{165}$ was added at the final concentration of 3 ng/ml. After 5 or 6 days, cells were trypsinized and counted. Values shown are means of duplicate determinations. The variation from the mean did not exceed 10%.

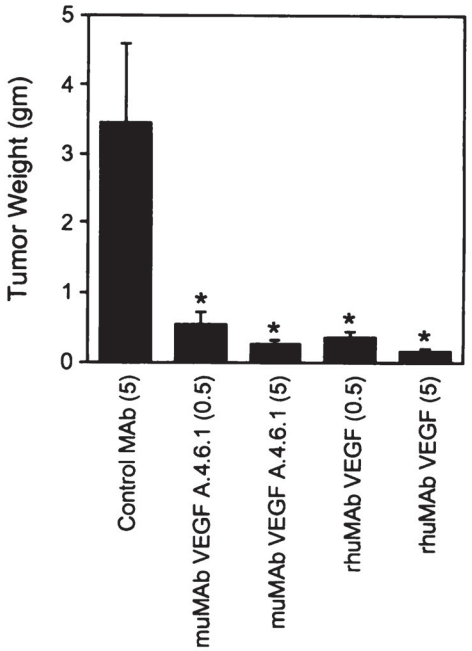

Fig. 4. Inhibition of tumor growth *in vivo*. A673 rhabdomyosarcoma cells were injected in BALB/c nude mice at the density of 2×10^6 per mouse. Starting 24 h after tumor cell inoculation, animals were injected with a control MAb, muMAb VEGF A.4.6.1, or rhuMab VEGF (IgG1) twice weekly, i.p. The dose of the control MAb was 5 mg/kg; the anti-VEGF MAbs were given at 0.5 or 5 mg/kg, as indicated ($n = 10$). Four weeks after tumor cell injection, animals were euthanized, and tumors were removed and weighed. *, significant difference when compared to the control group by ANOVA ($P < 0.05$).

ACKNOWLEDGMENTS

We thank K. Garcia for performing the VEGF binding ELISA, W. Henzel for protein microsequencing, A. Padua for amino acid analysis, J. Bourell for mass spectrometry, and J. Silva for animal studies. We are grateful to the DNA synthesis and the DNA sequencing groups at Genentech. We also thank C. Adams, J. Kim, B. Fendly, B. Keyt, and M. Beresini for helpful comments and advice.

REFERENCES

1. Folkman, J., and Shing, Y. Angiogenesis. J. Biol. Chem., *267:* 10931–10934, 1992.
2. Klagsbrun, M., and D'Amore, P. A. Regulators of angiogenesis. Annu. Rev. Physiol., *53:* 217–239, 1991.
3. Garner, A. Vascular diseases. *In:* A. Garner and G. K. Klintworth (eds.), Pathobiology of Ocular Disease. A Dynamic Approach, Ed. 2, pp. 1625–1710. New York: Marcel Dekker, 1994.
4. Weidner, N., Semple, P., Welch, W., and Folkman, J. Tumor angiogenesis and metastasis. Correlation in invasive breast carcinoma. N. Engl. J. Med., *324:* 1–6, 1991.
5. Horak, E. R., Leek, R., Klenk, N., Lejeune, S., Smith, K., Stuart, M., Greenall, M., and Harris, A. Quantitative angiogenesis assessed by anti-PECAM antibodies: correlation with node metastasis and survival in breast cancer. Lancet, *340:* 1120–1124, 1992.
6. Macchiarini, P., Fontanini, G., Hardin, M. J., Squartini, F., and Angeletti, C. A. Relation of neovascularization to metastasis of non-small cell lung carcinoma. Lancet, *340:* 145–146, 1992.
7. Good, D., Polverini, P., Rastinejad, F., Beau, M., Lemons, R., Frazier, W., and Bouck, N. A tumor suppressor-dependent inhibitor of angiogenesis is immunologically and functionally indistinguishable from a fragment of thrombospondin. Proc. Natl. Acad. Sci. USA, *87:* 6624–6628, 1990.
8. Clapp, C., Martial, J. A., Guzman, R. C., Rentier-Delrue, F., and Weiner, R. I. The 16-kilodalton N-terminal fragment of human prolactin is a potent inhibitor of angiogenesis. Endocrinology, *133:* 1292–1299, 1993.
9. O'Reilly, M. S., Holmgren, L., Shing, Y., Chen, C., Rosenthal, R. A., Mosem, M., Lane, W. S., Cao, Y., Sage, E. H., and Folkman, J. Angiostatin. A novel angiogenesis inhibitor that mediates the suppression of metastasis by a Lewis lung carcinoma. Cell, *79:* 315–328, 1994.
10. O'Reilly, M. S., Boehm, T., Shing, Y., Fukai, N., Vasios, G., Lane, W. S., Flynn, E., Birkhead, J. R., Olsen, B. R., and Folkman, J. Endostatin. An endogenous inhibitor of angiogenesis and tumor growth. Cell, *88:* 277–285, 1996.
11. Ferrara, N., and Davis Smyth, T. The biology of vascular endothelial growth factor. Endocr. Rev., *18:* 4–25, 1997.

12. Berkman, R. A., Merrill, M. J., Reinhold, W. C., Monacci, W. T., Saxena, A., Clark, W. C., Robertson, J. T., Ali, I. U., and Oldfield, E. H. Expression of the vascular permeability/vascular endothelial growth factor gene in central nervous system neoplasms. J. Clin. Invest., *91:* 153–159, 1993.
13. Brown, L. F., Berse, B., Jackman, R. W., Guidi, A. J., Dvorak, H. F., Senger, D. R., Connolly, J. L., and Schnitt, S. J. Expression of vascular permeability factor (vascular endothelial growth factor) and its receptors in breast cancer. Hum. Pathol., *26:* 86–91, 1995.
14. Brown, L. F., Berse, B., Jackman, R. W., Tognazzi, K., Manseau, E. J., Senger, D. R., and Dvorak, H. F. Expression of vascular permeability factor (vascular endothelial growth factor) and its receptors in adenocarcinomas of the gastrointestinal tract. Cancer Res., *53:* 4727–4735, 1993.
15. Mattern, J., Koomagi, R., and Volm, M. Association of vascular endothelial growth factor expression with intratumoral microvessel density and tumour cell proliferation in human epidermoid lung carcinoma. Br. J. Cancer, *73:* 931–934, 1996.
16. Dvorak, H. F., Brown, L. F., Detmar, M., and Dvorak, A. M. Vascular permeability factor/vascular endothelial growth factor, microvascular permeability and angiogenesis. Am. J. Pathol., *146:* 1029–1039, 1995.
17. Aiello, L. P., Avery, R., Arrigg, R., Keyt, B., Jampel, H., Shah, S., Pasquale, L., Thieme, H., Iwamoto, M., Park, J. E., Nguyen, H., Aiello, L. M., Ferrara, N., and King, G. L. Vascular endothelial growth factor in ocular fluid of patients with diabetic retinopathy and other retinal disorders. N. Engl. J. Med., *331:* 1480–1487, 1994.
18. Lopez, P. F., Sippy, B. D., Lambert, H. M., Thach, A. B., and Hinton, D. R. Transdifferentiated retinal pigment epithelial cells are immunoreactive for vascular endothelial growth factor in surgically excised age-related macular degeneration-related choroidal neovascular membranes. Invest. Ophthalmol. Visual Sci., *37:* 855–868, 1996.
19. Kim, K. J., Li, B., Houck, K., Winer, J., and Ferrara, N. The vascular endothelial growth factor proteins: identification of biologically relevant regions by neutralizing monoclonal antibodies. Growth Factors, *7:* 53–64, 1992.
20. Kim, K. J., Li, B., Winer, J., Armanini, M., Gillett, N., Phillips, H. S., and Ferrara, N. Inhibition of vascular endothelial growth factor-induced angiogenesis suppresses tumour growth *in vivo*. Nature (Lond.), *362:* 841–844, 1993.
21. Warren, R. S., Yuan, H., Matli, M. R., Gillett, N. A., and Ferrara, N. Regulation by vascular endothelial growth factor of human colon cancer tumorigenesis in a mouse model of experimental liver metastasis. J. Clin. Invest., *95:* 1789–1797, 1995.
22. Borgström, P., Hillan, K. J., Sriramarao, P., and Ferrara, N. Complete inhibition of angiogenesis and growth of microtumors by anti-vascular endothelial growth factor neutralizing antibodies. Novel concepts of angiostatic therapy from intravital videomicroscopy. Cancer Res., *56:* 4032–4039, 1996.
23. Melnyk, O., Schuman, M. A., and Kim, K. J. Vascular endothelial growth factor promotes tumor dissemination by a mechanism distinct from its effect on primary tumor growth. Cancer Res., *56:* 921–924, 1996.
24. Adamis, A. P., Shima, D. T., Tolentino, M., Gragoudas, E., Ferrara, N., Folkman, J., D'Amore, P. A., and Miller, J. W. Inhibition of VEGF prevents retinal ischemia-associated iris neovascularization in a primate. Arch. Ophthalmol., *114:* 66–71, 1996.
25. Miller, R. A., Oseroff, A. R., Stratte, P. T., and Levy, R. Monoclonal antibody therapeutic trials in seven patients with T-cell lymphoma. Blood, *62:* 988–995, 1983.
26. Schroff, R. W., Foon, K. A., Beatty, S. M., Odham, R. K., and Morgan, A. C., Jr. Human anti-murine immunoglobulin response in patients receiving monoclonal antibody therapy. Cancer Res., *45:* 879–885, 1985.
27. Neuberger, M. S., Williams, G. T., Mitchell, E. B., Jouhal, S. S., Flanagan, J. G., and Rabbits, T. H. A hapten-specific chimaeric IgE antibody with human physiological effector function. Nature (Lond.), *314:* 268–270, 1985.
28. Jones, P. T., Dear, P. H., Foote, J., Neuberger, M. S., and Winter, G. Replacing the complementarity-determining regions in a human antibody with those from a mouse. Nature (Lond.), *321:* 522–525, 1986.
29. Riechman, L., Clark, M., Waldmann, H., and Winter, G. Reshaping human antibodies for therapy. Nature (Lond.), *332:* 323–327, 1988.
30. Kabat, E. A., Wu, T. T., Perry, H. M., Gottesmann, K. S., and Foeller, C. Sequences of proteins of immunological interest, Ed. 5. Public Health Service, National Institutes of Health, Bethesda, MD, 1991.
31. Werther, W. A., Gonzalez, T. N., O'Connor, S. J., McCabe, S., Chan, B., Hotaling, T., Champe, M., Fox, J. A., Jardieu, P. M., Berman, P. W., and Presta, L. G. Humanization of an anti-lymphocyte function-associated antigen (LFA)-1 monoclonal antibody and reengineering of the humanized antibody for binding to rhesus LFA-1. J. Immunol., *157:* 4986–4995, 1996.
32. Carter, P., Presta, L., Gorman, C. M., Ridgway, J. B. B., Henner, D., Wong, W. L. T., Rowland, A. M., Kotts, C., Carver, M. E., and Shepard, H. M. Humanization of an anti-p185HER2 antibody for human cancer therapy. Proc. Natl. Acad. Sci. USA, *89:* 4285–4289, 1992.
33. Eigenbrot, C., Randal, M., Presta, L., and Kossiakoff, A. A. X-ray structures of the antigen-binding domains from three variants of humanized anti-p185HER2 antibody 4D5 and comparison with molecular modeling. J. Mol. Biol., *229:* 969–995, 1993.
34. Kunkel, T. A. Rapid and efficient site-specific mutagenesis without phenotypic selection. Proc. Natl. Acad. Sci. USA, *82:* 488–492, 1985.
35. Eaton, D. L., Wood, W. I., Eaton, D., Hass, P. E., Hollingshead, P., Wion, K., Mather, J., Lawn, R. M., Vehar, G. A., and Gorman, C. Construction, and characterization of an active factor VIII variant lacking the central one-third of the molecule. Biochemistry, *25:* 8343–8347, 1986.
36. Graham, F. L., Smiley, J., Russell, W. C., and Nairn, R. Characteristics of a human cell line transformed by DNA from human adenovirus type 5. J. Gen. Virol., *36:* 59–74, 1977.
37. Gorman, C. M., Gies, D. R., and McCray, G. Transient production of proteins using an adenovirus transformed cell line. DNA Prot. Eng. Tech., *2:* 3–10, 1990.
38. Lucas, B. K., Giere, L. M., DeMarco, R. A., Chisholm, V., and Crowley, C. W. High-level production of recombinant proteins in CHO cells using a dicistronic DHFR intron expression vector. Nucleic Acids Res., *24:* 1774–1779, 1996.
39. Chisholm, V. High efficiency gene transfer in mammalian cells. *In:* D. M. Glover and B. D. Hames (eds.), DNA Cloning 4. Mammalian systems, pp. 1–41. Oxford: Oxford University Press, 1996.
40. Park, J. E., Chen, H., Winer, J., Houck, K. A., and Ferrara, N. Placenta growth factor. Potentiation of VEGF bioactivity, *in vitro* and *in vivo,* and high affinity binding to Flt-1 but not to Flk-1/KDR. J. Biol. Chem., *269:* 25646–25645, 1994.
41. Karlsson, R., Roos, H., Fagerstam, L., and Persson, B. Kinetic and concentration analysis using BIA technology. Methods: A Companion to Methods in Enzymology, Vol. 6, pp. 97–108, 1994.
42. Leung, D. W., Cachianes, G., Kuang, W-J., Goeddel, D. V., and Ferrara, N. Vascular endothelial growth factor is a secreted angiogenic mitogen. Science (Washington DC), *246:* 1306–1309, 1989.
43. Presta, L. G., Lahr, S. J., Shields, R. L., Porter, J. P., Gorman, C. M., Fendly, B. M., and Jardieu, P. M. Humanization of an antibody directed against IgE. J. Immunol., *151:* 2623–2632, 1993.
44. Eigenbrot, C., Gonzalez, T., Mayeda, J., Carter, P., Werther, W., Hotaling, T., Fox, J., and Kessler, J. X-ray structures of fragments from binding and nonbinding versions of a humanized anti-CD18 antibody: structural indications of the key role of VH residues 59 to 65. Proteins, *18:* 49–62, 1994.
45. Chothia, C., Lesk, A. M., Tramontano, A., Levitt, M., Smith-Gill, S. J., Air, G., Sheriff, S., Padlan, E. A., Davies, D., Tulip, W. R., Colman, P. M., Spinelli, S., Alzari, P. M., and Poljak, R. J. Conformations of immunoglobulin hypervariable regions. Nature (Lond.), *342:* 877–883, 1989.
46. Xiang, J., Sha, Y., Jia, Z., Prasad, L., and Delbaere, L. T. Framework residues 71 and 93 of the chimeric B72.3 antibody are major determinants of the conformation of heavy-chain hypervariable loops. J. Mol. Biol., *253:* 385–390, 1995.
47. Tramontano, A., Chothia, C., and Lesk, A. M. Framework residue 71 is a major determinant of the position and conformation of the second hypervariable region in the VH domains of immunoglobulins. J. Mol. Biol., *215:* 175–182, 1990.
48. Fischmann, T. O., Bentley, G. A., Bhat, T. N., Boulot, G., Mariuzza, R. A., Phillips, S. E. V., Tello, D., and Poljak, R. J. Crystallographic refinement of the three-dimensional structure of the FabD1.3-lysozyme complex at 2.5-Å resolution. J. Biol. Chem., *266:* 12915–12920, 1994.
49. Baca, M., Presta, L. G., O'Connor, S. J., and Wells, J. A. Antibody humanization using monovalent phage display. J. Biol. Chem., *272:* 10678–10684, 1997.
50. Barbas, C. F., III. Selection and evolution of high-affinity anti-viral antibodies. Trends Biotechnol., *14:* 230–234, 1996.
51. Baselga, J., Tripathy, D., Mendelshon, J., Baughman, S., Benz, C. C., Dantis, L., Sklarin, N. T., Deidman, A. D., Hudis, C. A., Moore, J., Rosen, P. P., Twaddel, T., Henderson, I. C., and Norton, L. Phase II study of weekly intravenous recombinant humanized anti-p185^{HER2} monoclonal antibody in patients with HER2/neu overexpressing metastatic breast cancer. J. Clin. Oncol., *14:* 737–744, 1996.
52. von Mehren, M., and Weiner, L. M. Monoclonal antibody-based therapy. Curr. Opin. Oncol., *8:* 493–498, 1996.
53. Riethmuller, G., Schneider-Gadicke, E., and Johnson, J. P. Monoclonal antibodies in cancer therapy. Curr. Opin. Immunol., *5:* 732–739, 1993.